

Study on Various Finite Element Analysis on Concrete Filled Steel Tube Columns

Sandeep TN, Job Thomas

Department of Civil Engineering, School of Engineering, Cochin University of Science & Technology, Cochin, India

Department of Civil Engineering, School of Engineering, Cochin University of Science & Technology, Cochin, India

ABSTRACT: Concrete Filled Steel Tube Columns are found to be effective in terms of material utilization and there by sustainable development especially in high rise buildings. Numerical modeling of these columns using finite element software is an effective time saver while predicting their performance under loading. This paper summaries various finite element simulation techniques followed by researches in developing the models. The details included in the study covers the material properties of confined concrete and steel, element properties, the interface between tube and concrete, the initial imperfections both in steel tube as well in concrete, the effect of preloading and effect of partial loading etc.

KEYWORDS: Concrete-filled steel tube, CFST, Finite Element, Composite column.

I. INTRODUCTION

The use of composite structures being increased in recent years in construction industry, owing to the effective utilization of its materials. One such attempt was the introduction of Concrete Filled Steel Tube Columns (CFST Columns) in which rectangular or circular steel tubes are filled with concrete. The concrete infill delays the local buckling of the steel tube, while the steel tube provides confinement to the concrete infill. CFST columns impart better strength and ductility compared to conventional structural steel or reinforced concrete members. Also, the steel tube acts as a formwork for placing the concrete, which reduce the cost of construction. Schematic views showing applications of CFST columns in bridges and high-rise buildings are given in Fig. 1. Numerous studies were conducted to predict their behavior in the past, majority of them are experimental based. Numerical studies were also carried out by various researches, but less in number. Commercially available Finite Element Packages are being used to do the numerical analysis and their proper use makes the predictions correct. This leads to much economical designs of columns with less time. This paper reviews the various numerical finite element models that are develop in the past to predict the behavior of CFST columns in detail.

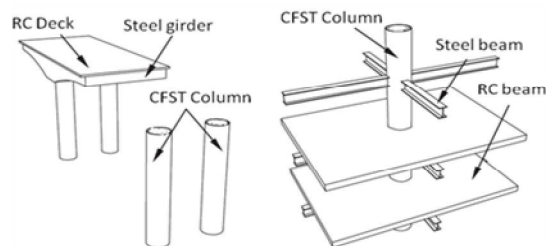


Fig. 1. Various applications of CFST columns

II. STUDY ON NUMERICAL MODELLING

It can be observed that majority of the analysis has been carried out using the software ABAQUS. Some researchers have used ANSYS to simulate the same. The modeling method adopted to simulate material properties, boundary conditions, interface, geometric imperfections, preloading and partial loading in these studies are summarized in the following sections.

A. MATERIAL PROPERTIES

The steel is taken as an elastic–plastic material with strain hardening in compression. A hardening rigidity of 2% E_s after yield may be adopted. The assumed stress–strain curve taken in [1] is shown in Fig. 2. The steel material behavior was defined using the Von Mises yield surface, associated flow rule, and kinematic hardening. The post-yield hardening modulus was assumed to be equal to $E_s/100$ [2]

Concrete may be treated as an elastic material until the confined strength is reached and then as plastic through the Drucker Prager option. The concrete material was modeled using the damaged plasticity material model in [2,3,4,5]. This model accounts for multi-axial behavior using a special compression yield surface to account for different evolution of strength in tension and compression. Typical stress strain relation used by [3,4] is shown in Fig. 3 and the relation in tension is shown in Fig. 4 which is used by [6].

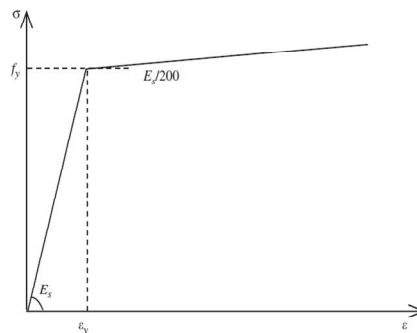


Fig. 2. Stress–strain curve for steel

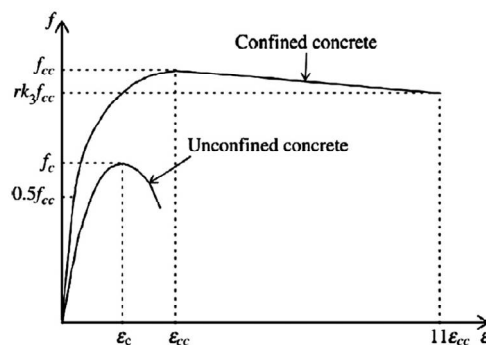


Fig. 3. Stress–strain curve for confined and unconfined concrete

The value of the dilation angle for unconfined concrete was 15° . Other researchers have reported using values between 15° and 30° . The default value of 0.1 was specified for the eccentricity ratio.

International Journal of Innovative Research in Science, Engineering and Technology

An ISO 3297: 2007 Certified Organization

Volume 5, Special Issue 14, December 2016

3rd National Conference on Recent Trends in Computer Science and Engineering and Sustainability in Civil Engineering (TECHSYNOD'16)

19th, 20th and 21st December 2016

Organized by

Department of CSE, MCA &CE, Mohandas College of Engineering and Technology, Thiruvananthapuram, Kerala, India

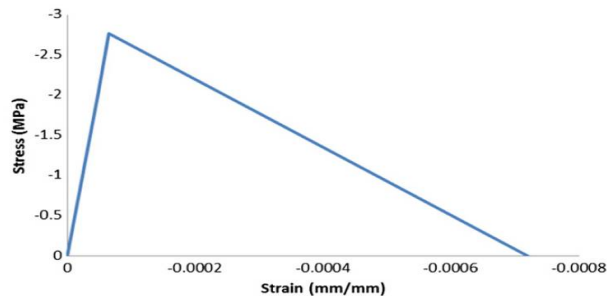


Fig. 4. Tensile Stress strain curve for confined concrete

The smeared cracking behavior in tension was specified using a stress vs. crack opening curve as shown in Fig. 5.

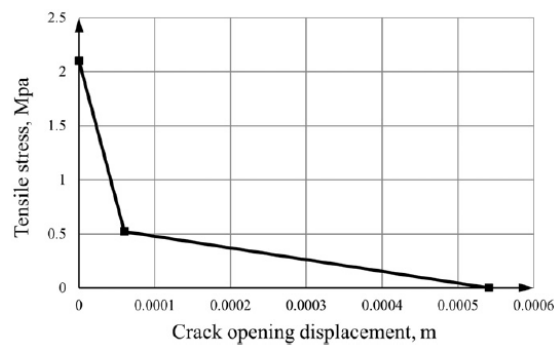


Fig. 5. Tensile stress-crack width based on CEB-FIP

B. Model and Boundary conditions

Because of symmetry of the specimens, only one-eighth of the column needs to be modeled, as shown in Fig. 6.

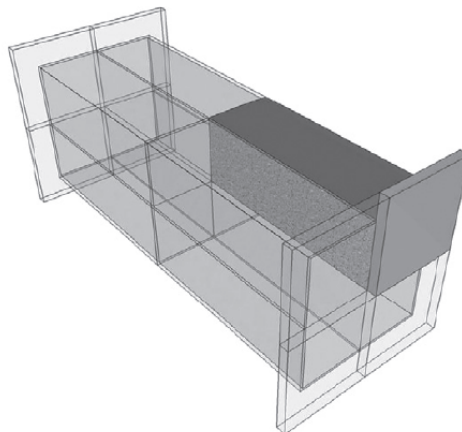


Fig. 6. Modeling only symmetrical region

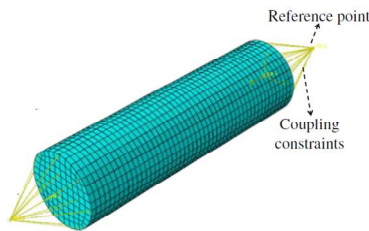


Fig. 7. Finite Element Model showing Boundary conditions

All the displacement degrees of freedom perpendicular to symmetric planes were to set zero using coupling restrained as shown in Fig 7. A rigid plate was used to simulate the end plate. Load was applied on the reference point as static uniform load using the displacement control.

C. ELEMENT PROPERTIES AND MESHING

In study [7], the steel shells were modeled as two layers of three dimensional quadratic solid elements C3D20R. The concrete adjacent to the steel walls was modeled as three dimension alquadratic solid elements C3D27R to avoid the intersecting of the concrete through the steel plate, and the rest of the concrete was modeled as C3D20R to reduce the run time. The rigid plate connected to the top of the steel box was modeled as three-dimensional rigid elements R3D4. These surfaces of the steel box and end plate were set as master surfaces and the concrete surfaces were set as slave surfaces. A reference point was set on the rigid plate at the position coincident with the center of the end plate. Compressive loading was applied through the reference point.

The steel tubes of the CFT members were modeled using a four-node S4R shell elements in [2,3,8]. These elements have: (i) six degrees of freedom per node, and (ii) five section points to compute the stress and strain variations through the thickness, and (iii) reduced integration in the plan of the elements. The elements model thick shell behavior, but converge to Kirchhoff's thin plate bending theory with reducing thickness. The concrete infill of CFT members was modeled using eight node solid elements with reduced integration (C3D8R). These elements have three degrees of freedom per node and reduced integration to calculate the stresses and strains in the elements. The C3D8R elements are computationally effective for modeling concrete cracking.

To select the proper FE mesh size that provides accurate results with minimum computational time, different mesh configurations are to be considered and the one which converge should select. The different mesh arrangement tried by [6] is shown in Fig. 8. In this, the fine meshes Mesh2 and Mesh3 converge to similar numerical results as compared with the course mesh (Mesh1), hence, Mesh2 was selected as it provides adequate accuracy and minimum computational time.

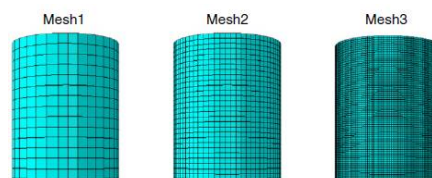


Fig. 8. Mesh convergence study

D. STEEL CONCRETE INTERFACE

Simulating the exact action of the interface between concrete and steel both at plastic and elastic stage is a difficult task. This contact were modeled in both the normal and tangential directions in [2,3]. The hard contact pressure-overclosure

relationship with penalty constraint method was used for interaction in the normal direction. The penalty friction formulation with coulomb friction coefficient equal to 0.55 [2], 0.6 [9] and maximum interfacial shear stress equal to 0.41 MPa was used for interaction in the tangential direction. There was no additional bond between the steel tube and the concrete infill in the model. The steel tube and concrete infill could slip relative to each other when the applied interfacial shear stress exceeded 0.55 times the contact pressure. Same Surface-based interaction with a contact pressure model in the normal direction and a Coulomb friction model in the tangential directions to the surface between steel tube and core concrete were used in [10]

The contact between the stainless steel stiffened tube and the concrete was modeled by interface elements in [11]. The interface elements consist of two matching contact faces of stainless steel stiffened tube and concrete elements. The friction between the two faces was maintained as long as the surfaces remained in contact. The coefficient of friction between the two faces is taken as 0.25 in the analysis. The interface element allows the surfaces to separate under the influence of tensile force. However, both contact elements were not allowed to penetrate each other.

E. GEOMETRIC IMPERFECTIONS

1) Steel tube: Initial imperfections in steel shells are inevitable and are to be considered while analyzing the column. Possible Local buckling was obtained by conducting an eigen value analysis on bare steel tubes (without any filling) [2,3,7]. The amplitude (magnitude) of the geometric imperfection was set equal to 0.1 times the steel tube thickness. First buckling eigen mode shape that has been used by [2,3] to define the geometric imperfection is shown in Fig. 9.

For columns with large slenderness, a lateral deflection of $L/1000$ at the mid-height was adopted to consider the global initial imperfection by [9]. These long columns suffer from initial imperfections. Hence, to include these imperfections in the simulation of slender columns, the modeling should consist of two steps as explained in [12]. In the first step, an elastic buckling analysis, called a linear perturbation analysis, was performed on a perfect slender column to obtain its buckling mode. Material plasticity strains and geometric imperfections, based on the first eigenmode, are then included. In the second step of the analysis to obtain the ultimate loads and the failure modes of the slender columns under axial compression. This is called the nonlinear analysis and it uses the modified RIKS method provided in ABAQUS.

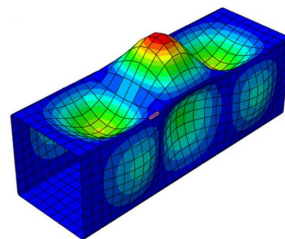


Fig. 9. Model showing imperfections in steel

2) Concrete: There are two types of gaps between concrete and steel tube; circumferential gap and spherical-cap gap, as shown in Fig. 10.

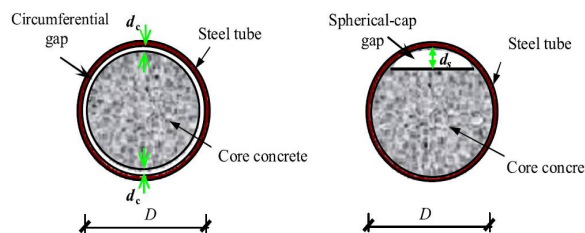


Fig. 10. Imperfection in Concrete

Circumferential gap is due to various reasons such as shrinkage of concrete temperature variation, negative confining force produced during the initial stage of CFST structures subjected to compression. Other one is due to poor construction practice.

For CFST with as pherical-cap gap, the shear stress at the interface between concrete and the steel tube will keep increasing with the increase of normal contact pressure until it exceeds the surface bond limit. After that, the relative slip is formed and the shear stress is then taken as constant. For a CFST with a circumferential gap has no direct contact with the inner surface of the steel tube at the initial stage. Therefore, both normal contact pressure and tangential shear stress are taken as zero at the beginning in the finite element model. Then after the contact occurs, the tangential frictional stress relies on the value of normal pressure stress [9,13].

F. PRELOADING AND PARTIAL LOADING

The steel columns are usually installed before inner concrete is placed. The steel columns are thus subjected to preload from constructional activities, self-weight of steel tubes and weight of wet concrete. The reload creates prestresses and deformation to the steel tubes, which would affect the load carrying capacity of the column.

In the FEA model [14], initially a preload was applied only on hollow steel tubes by deactivating concrete elements. In the second step, concrete elements were activated, analyzed with the initial deformations due to preload. The column was loaded until failure. During the second step, the preload was remained constant until column failure. The summation of the reaction force from boundary and preload was regarded as the capacity of composite column. The procedure adopted was shown in Fig. 11. Fig. 12 shows the vertical load (N) versus average longitudinal strain (e) under different preload ratios [14].

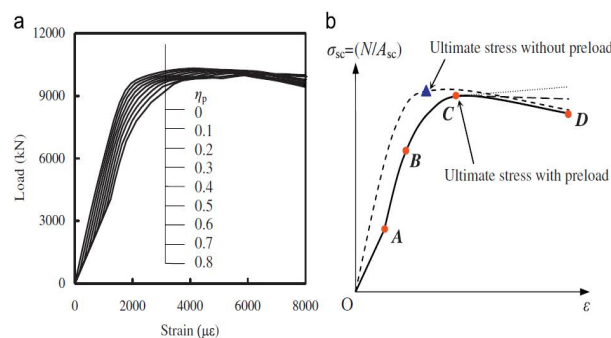


Fig. 11. Loading sequence showing preloading

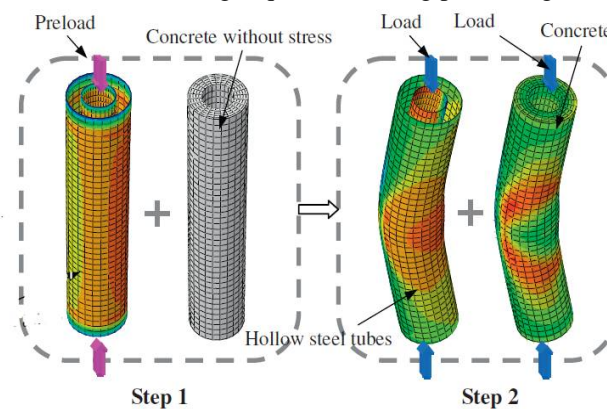


Fig. 12. Axial load Strain variation

It can be seen that generally four stages are presented for the columns with preload on tubes. 1. Preload stage (from point O to point A). During this stage, the preload is applied only on steel tubes. The initial deflection and longitudinal stress occur in the tubes. 2. Elastic stage (from point A to point B). The load is applied on the whole composite section, and the steel and concrete bear the load independently during this stage. The stiffness of the curve is comparable to that

Organized by

Department of CSE, MCA &CE, Mohandas College of Engineering and Technology, Thiruvananthapuram, Kerala, India

without preload on tubes. 3. Elastic-plastic stage (from point B to point C). The interaction will be generated between tubes and sandwiched concrete due to the different Poisson's ratio of two materials during this stage. The load increases with the deformation of the specimen, and the confinement provided by the outer steel tube is enhanced as well. When compared to the column without preload on tubes, the ultimate stress is smaller and the average strain corresponding to the ultimate stress is larger, for the confinement effect of steel tubes will be reduced with the preload. 4. Hardening or descending stage (from point C to point D). During this stage, the average stress will either increase or decrease due to the confinement effect of the outer tube.

CFST Columns may also be subjected to partial compression as in the case of a bridge pier having compressive load from bearings. A 'reference point' on the top surface of the bearing plate was set to model the hinge on the top by [15], and the boundary conditions for the were 'pinned', i.e. the translation components of reference point were restricted and the rotations of reference point were set free as shown in Fig. 13. The top surface of the bearing plate had the same translation and rotation components as those of the reference point. A uniform axial deformation was applied to the bottom surface of the composite columns, which was similar to the situation in the tests. The deformations were applied in several incremental steps, and the responses were calculated. The failure mode also shown in Fig. 13.

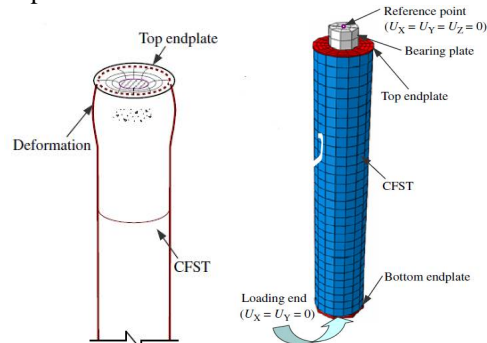


Fig. 13. Partial loading and failure mode

III. CONCLUDING REMARKS

Following conclusion can be drawn from the review of the studies conducted on CFST columns using finite element formulations. The exact behavior of CFST can be simulated using Finite Element software's with high level of accuracy. The initial imperfections, both in steel tube as well in concrete, the effect of preloading, effect of partial loading etc can be easily replicated using the numerical solution explained in this paper which is collected from the various recent previous studies.

REFERENCES

- [1] Lanhui Guo, Sumei Zhang, Wha-Jung Kim and Gianluca Ranzi, "Behavior of square hollow steel tubes and steel tubes filled with concrete," *Thin-Walled Structures*, vol. 45, pp. 961-973, July 2007.
- [2] Zhichao Lai and Amit H. Varma, "Noncompact and slender circular CFT members: Experimental database, analysis, and design," *Journal of Constructional Steel Research*, vol. 106, pp. 220-233, Nov 2014.
- [3] Zhichao Lai, Amit H. Varma and Kai Zhang, "Non-compact and slender rectangular CFT members: Experimental database, analysis, and design," *Journal of Constructional Steel Research*, vol. 101, pp. 455-468, June 2014.
- [4] M. Pagoulatou, T. Sheehan, X.H. Dai and D. Lam, "Finite element analysis on the capacity of circular concrete-filled double-skin steel tubular (CFDST) stub columns," *Engineering Structures*, vol. 72, pp. 102-112, April 2014.
- [5] M.F. Hassanein, O.F. Kharoob and L. Gardner, "Behaviour and design of square concrete-filled double skin tubular columns with inner circular tubes," *Engineering Structures*, vol. 100, pp. 410-424, June 2015.
- [6] Farid Abed, Mohammad AlHamaydeh and Suliman Abdalla, "Experimental and numerical investigations of the compressive behavior of concrete filled steel tubes (CFSTs)," *Journal of Constructional Steel Research*, vol. 80, pp. 429-439, Oct 2012.
- [7] Cheng-Cheng Chen, Jen-Wen Ko, Guo-Luen Huang and Ying-Muh Chang, "Local buckling and concrete confinement of concrete-filled box columns under axial load," *Journal of Constructional Steel Research*, vol. 78, pp.8-21, June 2012.
- [8] Burak Evirgen, Ahmet Tuncan and Kivanc Taskin, "Structural behavior of concrete filled steel tubular sections (CFT/CFST) under axial compression," *Thin-Walled Structures*, vol. 80, pp. 46-56, Feb 2014.
- [9] Fei-Yu Liao, Lin-Hai Han and Zhong Tao, "Behaviour of CFST stub columns with initial concrete imperfection: Analysis and calculations," *Thin-Walled Structures*, vol. 70, pp. 57-69, April 2013.

International Journal of Innovative Research in Science, Engineering and Technology

An ISO 3297: 2007 Certified Organization

Volume 5, Special Issue 14, December 2016

3rd National Conference on Recent Trends in Computer Science and Engineering and Sustainability in Civil Engineering (TECHSYNOD'16)

19th, 20th and 21st December 2016

Organized by

Department of CSE, MCA &CE, Mohandas College of Engineering and Technology, Thiruvananthapuram, Kerala, India

- [10] Fa-xing Ding, De-ren Lu, Yu Bai, Qi-shi Zhou, Ming Ni, Zhi-wu Yu and Guo-shuai Jiang, "Comparative study of square stirrup-confined concrete-filled steel tubular stub columns under axial loading," *Thin-Walled Structures*, vol. 98, pp. 443-453, Oct 2015.
- [11] Ehab Ellobody, "Nonlinear behavior of concrete-filled stainless steel stiffened slender tube columns," *Thin-Walled Structures*, vol. 45, pp. 259-273, Feb 2007.
- [12] M.F. Hassanein and O.F. Kharoob, "Analysis of circular concrete-filled double skin tubular slender columns with external stainless steel tubes," *Thin-Walled Structures*, vol. 79, pp. 23-37, Jan 2014.
- [13] Jun-Qing Xue, Bruno Briseghella and Bao-Chun Chen, "Effects of debonding on circular CFST stub columns," *Journal of Constructional Steel Research*, vol. 69, pp. 64-76, Aug 2011.
- [14] Wei Li, Lin-Hai Han and Xiao-Ling Zhao, "Axial strength of concrete-filled double skin steel tubular (CFDST) columns with preload on steel tubes," *Thin-Walled Structures*, vol. 56, pp. 9-20, March 2012.
- [15] Y.F. Yang and Lin-Hai Han, "Concrete filled steel tube (CFST) columns subjected to concentrically partial compression," *Thin-Walled Structures*, vol. 50, pp. 147-156, Sep 2011.